Synthesis of Nano-Structured Stainless Steel Powder by Mechanical Alloying and Characterization

A THESIS SUBMITTED IN PARTIAL FULLFILLMENT

OF THE REQUIREMENT FOR THE DEGREE OF

Bachelor of Technology

In

Metallurgical and Materials Engineering

By

BIBHU PRASAD BEHERA (109MM0437)

SAROJ KUMAR JENA (109MM0470)

DEPARTMENT OF METALLURGICAL AND MATERIALS ENGINEERING

NATIONAL INSTITUTE OF TECHNOLOGY, ROURKELA

Batch (2009-2013)

Synthesis of Nano-Structured Stainless Steel powder by Mechanical Alloying and Characterization

A THESIS SUBMITTED IN PARTIAL FULLFILLMENT

OF THE REQUIREMENT FOR THE DEGREE OF

Bachelor of Technology

In

Metallurgical and Materials Engineering

By

BIBHU PRASAD BEHERA (109MM0437)

SAROJ KUMAR JENA (109MM0470)

UNDER THE GUIDANCE OF

DR. DEBASIS CHAIRA

DEPARTMENT OF METALLURGICAL AND MATERIALS ENGINEERING

NATIONAL INSTITUTE OF TECHNOLOGY, ROURKELA

May, 2013

National Institute of Technology

Rourkela

Certificate

This is to certify that the thesis entitled "**Synthesis of Nano-Structured Stainless Steel powder by Mechanical Alloying and Characterization**" being submitted by Bibhu Prasad Behera (109MM0437) and Saroj Kumar Jena (109MM0470) for the partial fulfillment of the requirements of Bachelor of Technology degree in Metallurgical and Materials engineering is a bona fide thesis work done by them under my supervision during the academic year 2012-2013, in the Department of Metallurgical and Materials Engineering, National Institute of Technology Rourkela, India.

The results presented in this thesis have not been submitted elsewhere for the award of any other degree or diploma.

Date: 9/5/2013

(Dr. Debasis Chaira)

Metallurgical and Materials Engineering

National Institute of Technology Rourkela

Rourkela-769008, Odisha, India

Acknowledgment

We would like to express our sincere gratitude to our guide Dr. Debasis Chaira, Metallurgical and Materials Engineering, NIT Rourkela, for giving the opportunity to work with him and also providing excellent guidance and continuous assistance throughout the project work. His constant criticism, advice, assertions, appreciation were very vital and irrevocable, giving us that boost without which it wouldn't have been possible for us to finish our project. There's not a single day we can remember during our work days which went by without his scrutiny and guidance. We have received endless support and guidance from him, right from the development of ideas, deciding the experiments and methodology of work and this presentation. We are thankful to him for his encouragement throughout the project .We wish to express our deep sense of gratitude to Prof. B.C. Ray, HOD, Metallurgical and Materials Engineering, NIT Rourkela for giving us an opportunity to work on this project. We would be highly obliged to extend our thanks to The PH.d Scholar Mr. Shashanka R for his immense support and help rendered while carrying out our experiments, without which the completion of this project would have been impossible. We would also like to thank all the staff members of MME Dept., NITR and everyone who in some way or the other has provided us valuable guidance, suggestion and help for this project.

Date: 9/5/2013

Bibhu Prasad Behera (109MM0437)

Saroj Kumar Jena (109MM0470)

Metallurgical and Materials Engineering

National Institute of Technology
Rourkela-769008

Abstract

In the present work, nano-structured ferritic and austenitic stainless steel powders were prepared by mechanical alloying for a period of 10 hours in a high energy planetary ball mill. An austenitic stainless steel composition containing elemental powders of 18%Cr - 13%Ni – Fe and for ferritic stainless steel of 17%Cr -1%Ni – Fe were milled in a specially designed high energy planetary mill under toluene. The effect of stearic acid on synthesis stainless steel was observed during mechanical alloying. The samples were taken out from the ball mill in the intervals of 0 hours, 30 minutes, 2 hours, 5 hours and 10 hours. Then the powders were characterized by X-ray diffraction, scanning electron microscopy and particle size analysis to get brief idea about the nano-structured stainless steel produced and to determine the phase transformation and microstructural morphology. The crystallite size and strain was determined by using Williamson-Hall method. The lattice parameter of the particle was calculated by using Nelson-Riley function. By using stearic acid the crystallite size of austenitic stainless steel changes from 124.63nm to 6.1nm and for ferritic stainless steel it changes from 120.70 nm to 8.47 nm after 10 hours of milling. The lattice strain continuously increases with milling in both cases. It has been found that stearic acid prevent agglomeration of particles and hinders phase transformation to some extent due to formation of layer on particle surface as it prevent diffusion. It also has been noticed that stearic acid prevents the strain hardening of the powder particles.

Keywords:

Stainless steel, mechanical alloying, X-Ray Diffraction, Scanning Electron Microscope and particle size analysis

CONTENTS

List of figures

1. Introduction

Stainless steel are stainless as these have a minimum of 11.5% chromium in them, which having more affinity for oxygen than iron has, forms a very thin, protective and stable (probably Cr_2O_3) film on the surface. The film is continuous, impervious and passive to stop further reaction between the steel and surrounding atmosphere. Thus, chromium imparts to the steels corrosion resistance, oxidation resistance and pleasing appearance. Apart from this essential element chromium, the stainless steels have also addition of nickel, molybdenum and manganese to enhance other properties and improve the corrosion resistance.

Stainless steel could be divided into 5 categories:

- Ferritic Stainless Steel
- Austenitic Stainless Steel
- Martensitic Stainless Steel
- Duplex Stainless Steel
- Precipitation-hardenable Stainless steel

Among these 5 types of stainless steel, ferritic and austenitic stainless steels are very important and used in various applications. Ferritic stainless steels are iron-chromium alloys having chromium 11.5 to 27%, but usually between 17 to 26%. These are ferritic structure up to melting point. The carbon content as low as possible to improve toughness and reduce sensitization. Molybdenum is used to increase the corrosion resistance particularly pitting and local corrosion. Niobium and titanium are used to steels to stabilize against intergranular corrosion. As expensive nickel is not added to ferritic stainless steel as it is cheaper than austenitic stainless steel. These steels have reasonable cold formability. They have excellent hot ductility. Ferritic stainless steels, in general, are not as readily deep drawn as austenitic alloys because of the overall lower ductility. However, they are suitable for other deformation processes such as spinning and cold forging. They have good machinability, higher thermal conductivity and lower thermal expansion than austenitic stainless steel. They are magnetic in nature.

Austenitic stainless steel having (16-25) % chromium and sufficient amount of austenite stabilizing elements like nickel, manganese or nitrogen. So that the steels are austenitic at room

temperature, are called austenitic stainless steel. As the nickel content increases in steel, the amount austenite present at the solution-treatment temperature increases and the M_s temperature is lowered, so that 8% nickel, the M_s temperature is just below room-temperature. These steels are non-magnetic in nature. They are tough even at low temperature as there is no ductile to brittle transition temperature. They have good ductility with elongation of about 50% in tensile tests. These steels do not have '475^0C' embrittlement. Austenitic stainless steels have low yield stress, relatively high ultimate tensile strength and high ductility, when compared to a typical carbon steel.

Stainless steel powder is widely used in offshore applications as it has excellent corrosion resistance property. Typical applications of stainless steel powder are-

- Sintered Metallic Filters
- Anti-Corrosive Paintings
- Thermal Spray Coatings
- Consolidated Products By HIP

Typical stainless steel components used in offshore applications are-valve body, elbow raiser and mixer house. A range of components are available for applications with oil and gas, power generation and general engineering sectors.

The effect of the alloying elements on the microstructure of the stainless steels can be understood by Schaeffler diagram. Fig. 1 shows the schematic of Schaeffler diagram.

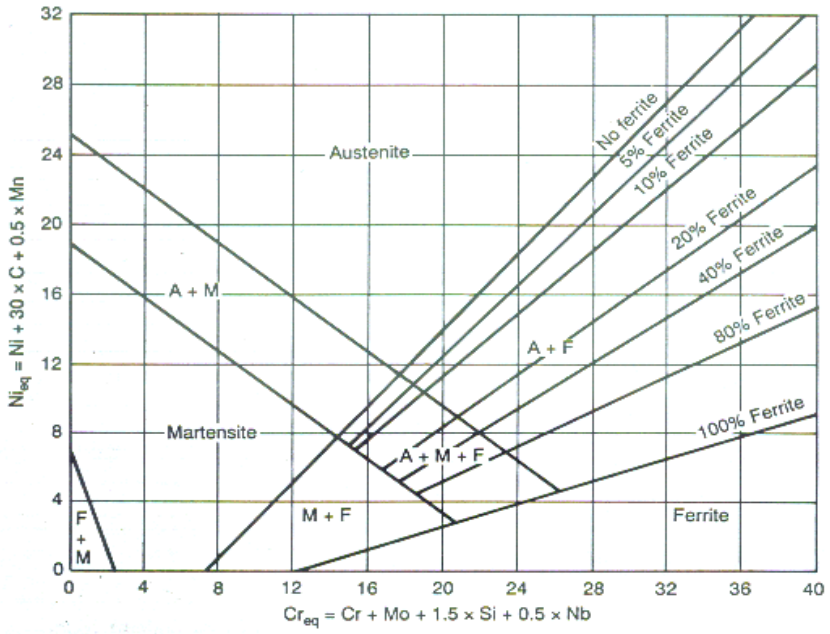

Fig. 1.1 Schaeffler diagram

This diagram illustrates the phases present at function of nickel equivalent and chromium equivalent. Nickel equivalent is determined by austenite stabilizing elements such as:

Ni equivalent= Ni + Co + 0.5(Mn) +0.3 (Cu) +25 (N) + 30 (C)

Chromium equivalent is determined by Ferritic stabilizing elements such as:

Cr equivalent= Cr + 2 (Si) +1.5 (Mo) +5 (V) +5.5 (Al) +1.75 (Nb) + 1.5 (Ti) + 0.75 (W)

Among the different processes able to produce nano-crystalline powders in bulk quantities, high-energy milling is one of the most interesting from an industrial point of view. High-energy milling of nano phase powders is one of the less sophisticated technologies-and, in such a sense, also the most inexpensive-to produce nano phase powders; in fact, it exploits devices and processes that have many aspects in common with mixing, fine grinding, and comminution of materials. However, it does have interest for applications, as, in principle, this is very low cost process and its potential for industrial applications is very significant.

The concept of high-energy milling process is very simple: to seal in a vial some-usually powdered-materials along with grinding media, which are usually balls, and to reduce the size of the materials by mechanical activation, providing at the same time an intimate mixing of the different materials introduced, so close that diffusion, and chemical reactivity are greatly enhanced.

1.1 Objective

The main objectives of the present study are as:

- Synthesis of austenitic and ferritic stainless steel powder from elemental powder composition by mechanical alloying
- Feasibility study of formation of nanostructure
- Synthesis of bulk amount powder in less milling time
- Characterization of the powder to evaluate crystal size, lattice strain, particle size and morphology and lattice parameter

1.2 Scope of the project

The chapter one gives the detailed introduction of the project and describes the process of mechanical alloying. It also gives a brief idea about the importance and applications stainless steel. The main objectives of the present study are also highlighted here. Chapter two gives the literature review related to the project. Chapter three give a brief idea of the experimental procedure followed. It includes details of milling experiments and milling parameters used. This chapter tells us about the characterization techniques used to determine the crystallite size, strain, lattice parameter and powder morphology. Chapter four describes results and discussions.

2. Literature survey

Mechanical alloying (MA) is a solid-state powder processing technique involving repeated welding, fracturing, and re-welding of powder particles in a high-energy ball mill.

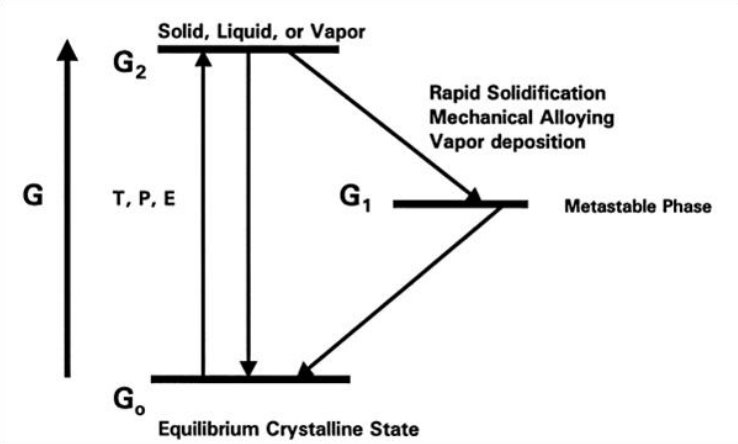

Fig. 2: The basic concept of "energizing and quenching" to synthesize non-equilibrium particles

MA has now been shown to be capable of synthesizing a variety of equilibrium and non-equilibrium alloy phases starting from blended elemental or pre-alloyed powders. The non-equilibrium phases synthesized include supersaturated solid solutions, metastable crystalline and quasicrystalline phases, nanostructures, and amorphous alloys.

Recent advances in these areas and also on disordering of ordered intermetallics and mechanochemical synthesis of materials have been critically reviewed after discussing the process and process variables involved in MA.

The often vexing problem of powder contamination has been analyzed and methods have been suggested to avoid/minimize it. The present understanding of the modelling of the MA process is also under research.

Attributes of mechanical alloying

- Production of fine dispersion of second phase particles (usually oxide)
- Extension of solid solubility limits
- Refinement of grain sizes down to nanometer range
- Synthesis of novel crystalline and quasi crystalline phases
- Development of amorphous (glassy) phases
- Disordering of ordered intermetallics
- Possibility of alloying of difficult to alloy elements
- Inducement of chemical (displacement) reaction at low temperatures
- Scaleable process

Process variables

MA is a complex process and hence involves optimization of a number of variables to achieve the desired product phase and/or microstructure. Some of the important parameters that have an effect on the final constitution of the powder are:

- Type of mills
- Milling container
- Milling speed
- Milling time
- Type, size and size distribution of the grinding medium
- Ball to powder ratio
- Extent of filling the vial
- Milling atmosphere
- Process control agent
- Temperature of milling

Mechanism of mechanical alloying

During high-energy milling the powder particles are repeatedly flattened, cold welded, fractured and re-welded. Whenever two steel balls collide, some amount of powder is trapped in between them. Typically, around 1000 particles with an aggregate weight of about 0.2 mg are trapped during each collision. The force of the impact plastically deforms the powder particles leading to work hardening and fracture. The new surfaces created enable the particles to weld together and this leads to an increase in particle size. Since in the early stages of milling, the particles are soft (if we are using either ductile-ductile or ductile-brittle material combination), their tendency to weld together and form large particles is high. A broad range of particle sizes develops, with some as large as three times bigger than the starting particles. The composite particles at this stage have a characteristics layered structure consisting of various combinations of starting constituents. With continued deformation, the particles get work hardened and fracture by a fatigue failure mechanism and/or by the fragmentation of fragile flakes. Fragments generated by this mechanism may continue to reduce in size in the absence of strong agglomeration forces. At this stage, the tendency to fracture predominates over cold welding. Due to continuous impact of grinding balls, the structure of the particles is steadily refined, but the particle size continuous to be same. Consequently, the inter-layer spacing decreases and the number of layers in a particle increase. However, it should be remembered that the efficiency of particles size reduction is very low, about 0.1% in a conventional ball mill. The efficiency may be somewhat higher in high-energy ball milling process, but is still less than 1%. The remaining energy is lost mostly in form of heat, but a small amount is also utilized in the elastic and plastic deformation of the powder particles. After milling for a certain length of time, steady-state equilibrium is attained when a balance is achieved between the rate of welding, which tends to decrease the average composite particle size. Smaller particles are able to withstand deformation without fracturing and tend to be welded into larger pieces, with an overall tendency to drive both very fine and large particles towards an intermediate size. At this stage each particle contains substantially all of the starting ingredients, in the proportion they were mixed together and the particles reach saturation hardness due to the accumulation of strain energy. The particle size distribution at this stage is narrow, because particles larger than average are reduced in size at the same rate that fragments smaller than average grow through agglomeration of smaller particles.

From the forging it is clear that MA, heavy deformation is introduced into the particles. This is manifested by the presence of variety of crystal defects such as dislocations, vacancies, stacking faults and increased number of grain boundaries. The presence of this defect structure enhances the diffusivity of solute elements into matrix. Further, the refined microstructural features decrease the diffusion distances. Additionally, the slight increase in temperature during milling further aids the diffusion behavior and consequently, true alloying takes place amongst the constituent elements. While this alloying generally takes place nominally at room temperature, sometimes it may be necessary to anneal the mechanically alloyed powder at an elevated temperature for alloying to be achieved. This is particularly true when formation of intermetallics is desired.

The specific times required to develop a given structure in any system world be a function of the initial particle size and characteristics of the ingredients as well as the specific equipment used for conducting the MA operation and the operating parameters of the equipment. But, in most of the cases, the rate of refinement of the internal structure (particle size, crystallite size, lamellar spacing, etc.) is roughly logarithmic with processing time and therefore the size of the starting particles is relatively unimportant. In a few minutes to an hour, the lamellar spacing usually becomes small and the crystallite (grain) size is refined to nanometer ($1nm=10^{-9}m$ or $10A^{0}$) dimensions. The ease with which nano-structured materials can be synthesized is one reason why MA has been extensively employed to produce nano-crystalline materials. As mentioned above, it is possible to conduct MA of three different combinations of metals and alloys:

- Ductile-ductile system
- Ductile-brittle system
- Brittle-brittle system

Enayati *et al.* 2007 [1] showed that when Fe–18Cr–8Ni and Fe–15Cr–15Ni elemental powder is alloyed mechanically, leads to the formation of a single-phase BCC solid solution of martensite with nanoscale size grains of almost 15 nm. They observed that heat treatment of mechanical alloyed powder at $700^{0}C$ leads to formation of dual structure consisting of austenitic and martensitic phases. But the structure of Fe–15Cr–25Ni powder after milling remains as it is even

after isothermal annealing resulting in the fully austenitic structure. Oleszak *et al.* 2006 [2] synthesized 316L austenitic steel powders in a planetary Fritsch P5 mill and found two-phase structures consisting of austenitic and martensitic stainless steel. Both the phases demonstrated nanocrystalline nature of crystallite size in the range 10–20 nm. After a very short period of milling, the martensite content reached to 66%. As the milling time increases, the content of martensite decreases. This resulted in the formation stable nanocrystalline austenitic stainless steel powder. Sintering was done by pulse current sintering technique to get dense hardened samples having austenitic nature. Sherif El-Eskandarany *et al.* 1994 [3] studied the synthesis of Fe-18Cr-8Ni elemental powder in rod mill at room temperature. After 1080ks of milling, they obtained homogeneous amorphous phase of austenitic stainless steel powder. They studied thermal behavior, structural morphology successfully. During first 2ks of milling, the elemental particles of Fe, Cr and Ni would not form any composition material. But as the milling time increases, they observed agglomeration of the particles starts resulting in the increased particle size up to 50ks and becomes spherical and nanocrystalline after prolonged milling. Haghir *et al.* 2009 [4] studied the phase transformation of ferritic to austenitic structure. They also studied the effect of argon and nitrogen gases on the structure of stainless steel using the elemental composition of Fe–18Cr–11Mn. They concluded their findings by showing argon gas atmosphere favours formation of ferritic stainless steel powder and nitrogen gas atmosphere favours austenitic stainless steel powder after 120 h and 100 h respectively. They analyzed the variation of nitrogen content with milling time and they concluded that, the solubility of nitrogen increases with increase in milling time at N_2 atmosphere and it reaches as high as 0.65wt% after 100h.

3. Experimental Details

Two alloy compositions of 18%Cr - 13%Ni – Fe (wt. %) and 17%Cr -1%Ni – Fe (wt. %) were mechanical alloyed for 10 h in a specially designed dual-drive planetary mill. Milling was conducted under toluene to prevent oxidation. One jar contains austenitic stainless steel powder (18%Cr - 13%Ni – Fe) and another jar contains ferritic stainless steel powder (17%Cr -1%Ni – Fe). In one set of experiment milling was conducted with stearic acid (2 wt. % of powder) and in another set without stearic acid. In both cases, a ball to powder ratio of 6:1 was maintained. The total weight of the balls (8 mm diameter) used was 1Kg. The samples were taken out from the mill at the time intervals of 0.5 hours, 2 hours, 5 hours and 10 hours to study phase transformation, particle morphology and size change during mechanical alloying. The powders were characterized by scanning electron microscopy (SEM), x-ray difffractometer (XRD) with CuK_{α} target and particle size analysis. Then crystallite size and lattice strain were calculated from XRD peak broadening by using Williamson-Hall equation. The lattice parameter of the particle was also calculated by using Nelson-Riley function.

Table 3.2: Summary of milling parameters used

Parameter	Value
Balls/powder ratio	6:1
Ball diameter	8 mm
Atmosphere	Air
Grinding medium	wet (Toluene)
Weight of powder	166.6 gm.
Milling time	10 hrs.(pause mode every 30 min)
Type of mill	High energy ball mill
Milling speed	300rpm

4. Results and Discussions

Characterization of mechanically alloyed powders

The mechanically alloyed powders were analyzed by X-Ray Diffraction, SEM and particle size analysis to understand the topographical characteristics and get information about elements and phases present in the powder after different hours of milling. Crystallite size and strain of the milled powders were calculated by using Williamson-Hall Equation. The lattice parameter of the powder was also calculated by using Nelson-Riley function.

4.1 X- Ray Diffraction analysis

X-ray diffraction (XRD) characterization were carried out for identification and phase evolution at different stages of milling by using the Cu-Kα radiation (having wavelength of 0.1789 nm) in a Phillip's X'pert PRO high resolution X-ray diffratometer. The X-ray source was operated at a voltage of 40 kV and current of 35 mA. The diffraction angle was varied in the range of 20-100 degrees while the scanning rate was 0.05°/s. The crystallite size and lattice strain were estimated by measuring the broadening of the X-ray peaks by using Williamson- Hall plot. The lattice parameter of the particle is also calculated by using Nelson-Riley function.

4.1.1 General Interpretation of diffraction patterns

Fig. 4.1 and Fig. 4.2 shows the XRD patterns of austenitic and ferritic stainless steel powder milled for different time periods respectively (without stearic acid). From the graphs it is observed that iron, nickel and chromium were present during the initiation of milling. Many observations were obtained from these diffraction patterns for the structural characterization of the powder at different stages of milling. The most important observation is that all the peaks tend to broaden as milling time increases. The peak broadening is due to grain refinement and increase of lattice strain. Secondly, we observed that as milling time increases, the peaks for nickel and chromium decreases and at the end of 10 hours the peaks almost disappear. The

reduction and disappearance of the Ni and Cr peaks in the XRD patterns suggests that the Cr and Ni particles are getting diffused inside the lattice of and causes the formation of solid solution. It is clear from XRD spectra that there is formation of austenite phase along with ferrite phase in case of austenitic stainless steel. However, in case of ferritic stainless steel all peaks correspond to ferrite.

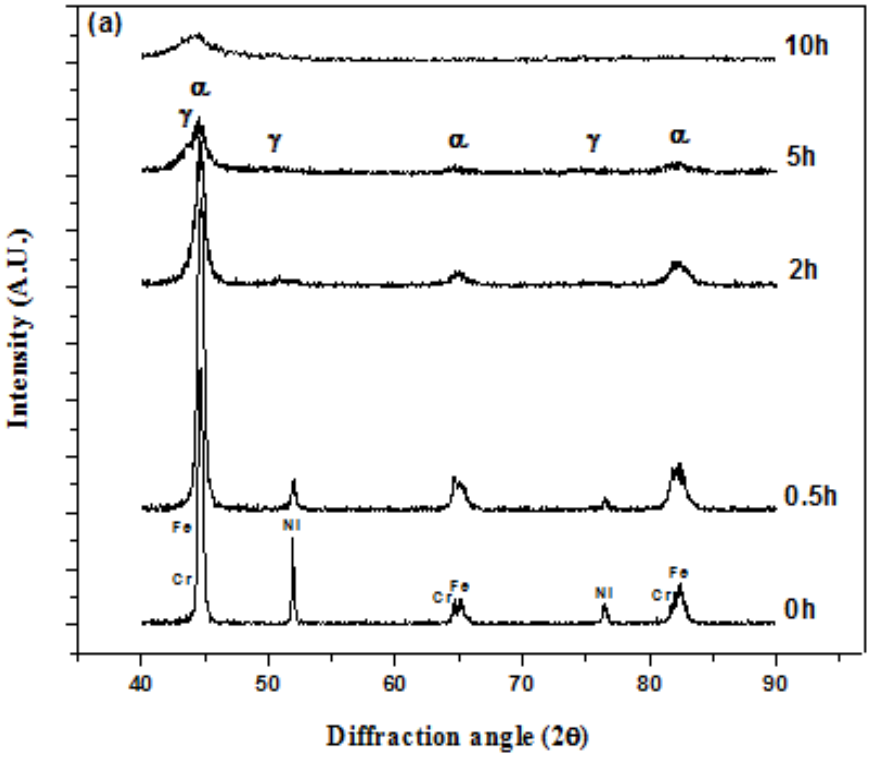

Fig. 4.1: XRD results of austenitic stainless steel (18%Cr - 13%Ni – Fe) powder at different milling hours (without stearic acid)

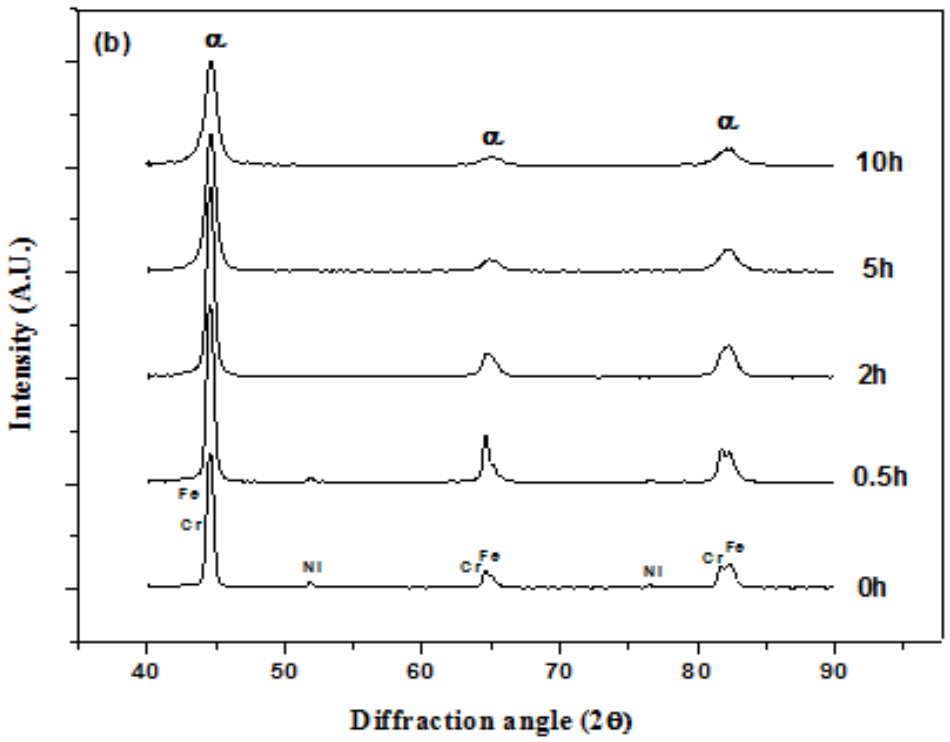

Fig. 4.2: XRD results of ferritic stainless steel powder (17%Cr -1%Ni – Fe) at different milling hours (without stearic acid)

Figure 4.3 and Figure 4.4 shows the XRD patterns of austenitic and ferritic stainless steel powder milled for different time periods respectively (with stearic acid, 2 wt. %). From the graphs it is known that iron, nickel and chromium were present at 0 hours or during the initiation of milling. Many observations were obtained from these diffraction patterns for the structural characterization of the powder at different stages of milling. The most important observation is that all the peaks tend to broaden as milling time increases. Secondly, we observed that as milling time increases the peaks for nickel and chromium decreases but did not disappears at the end of 10 hours. This occurs due to the presence of stearic acid which prevents agglomeration by forming a layer on the steel powder. Presence of stearic acid could be the cause of the delays phase transformation as it forms a layer on powder surface and prevents diffusion to some extent. The reduction in intensity of the Ni and Cr peaks in the XRD patterns suggests that the Cr and Ni particles are getting diffused inside the lattice of and causes the formation of solid solution.

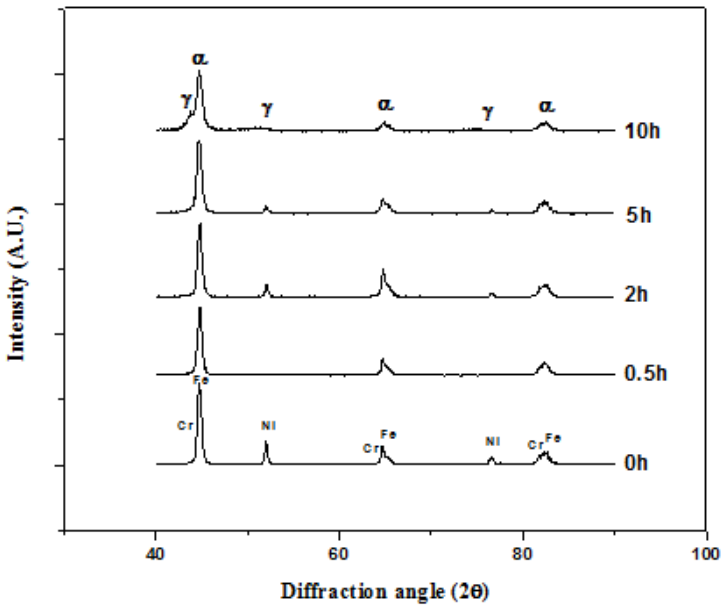

Fig. 4.3: XRD results of austenitic stainless steel powder samples at different milling hours (with stearic acid)

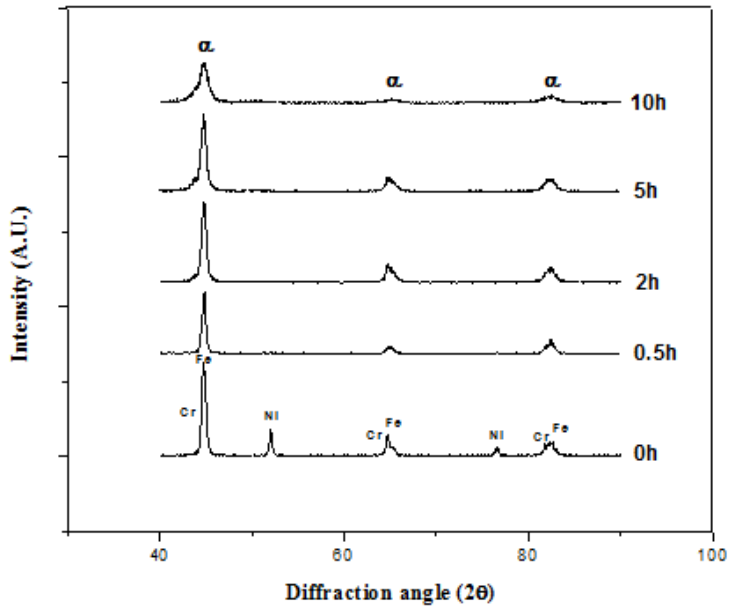

Fig. 4.4: XRD results of ferritic stainless steel powder samples at different milling hours (with stearic acid)

4.1.2 Crystallite size and lattice strain calculation

XRD results were used to calculate the crystallite size and lattice strain by using Williamson-Hall Equation which is given by (equation 1):

$$\beta \cos\theta = {}^{0.94\boldsymbol{\lambda}}/_{D} + 4\eta \sin\boldsymbol{\theta} \qquad (1)$$

Where,

β = Full width Half Maxima

η = strain

λ = wavelength

D = Crystallite Size

In order to calculate the crystallite size and lattice strain, graph was plotted as βcosθ in y axis and sinθ in x axis. From the graph, a straight line is obtained. Then the slope and intercept of the straight line was calculated.

Fig. 4.5 and Fig. 4.6 show the variation of crystallite size and strain of the austenitic and ferritic stainless steel powder with milling time (without stearic acid). We found that as milling time increases the crystallite size decreases and after certain milling duration it tends to achieve a stable value and on further milling the change in crystal size become very less. On the other hand, with the increase in milling time the lattice strain increases. It should be noted that in case of austenitic stainless steel, crystal size and lattice strain can't be measured after 10 hours as only one peak is present.

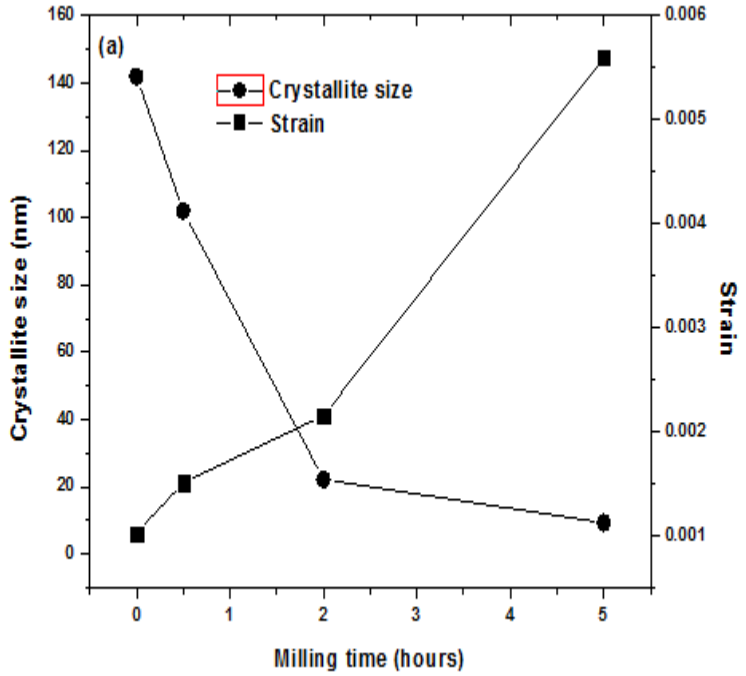

Fig. **4.5: Graph showing variation of crystallite size and lattice strain with milling time of austenitic stainless steel (without stearic acid)**

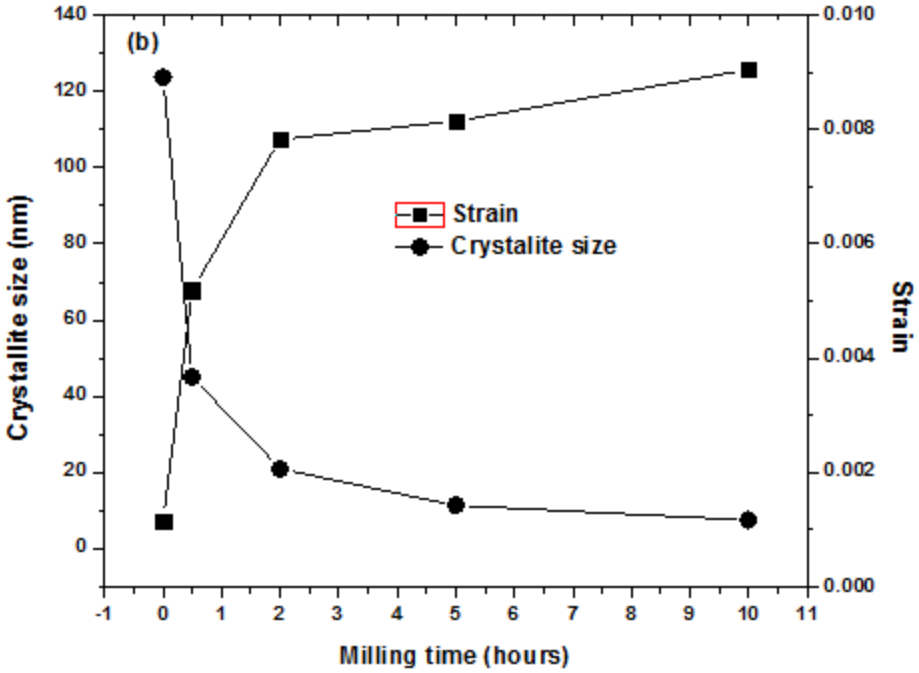

Fig. 4.6: Graph showing variation of crystallite size and lattice strain with milling time of ferritic stainless steel (without stearic acid)

Fig. 4.7 and Fig. 4.8 show the variation of crystallite size and strain of the austenitic and ferritic stainless steel powder with milling time(with stearic acid). The both graphs show similar behavior as without stearic acid.

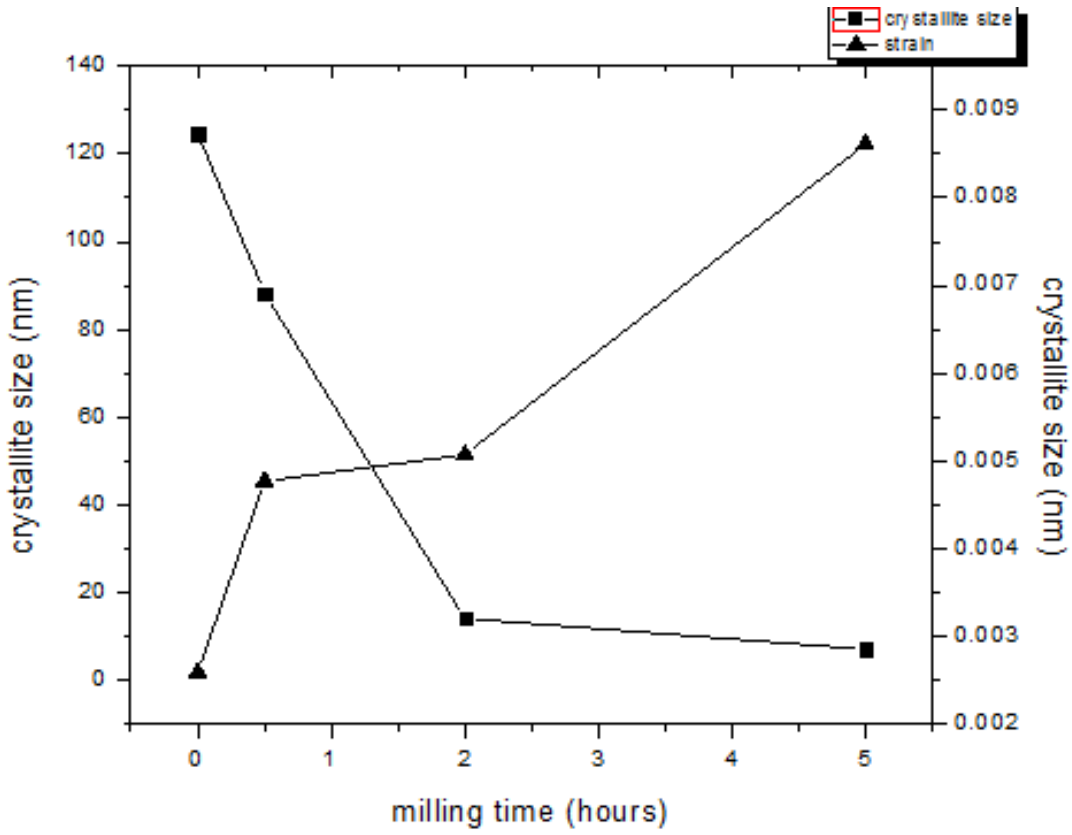

Fig. 4.7: Graph showing variation of crystallite size and lattice strain with milling time of austenitic stainless steel (with stearic acid)

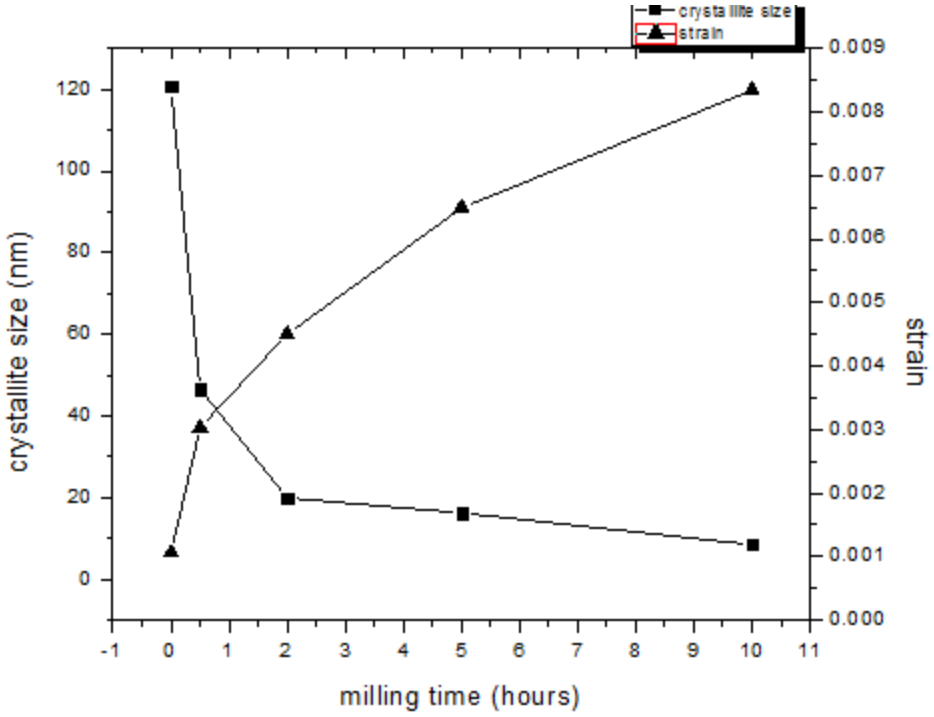

Fig. 4.8: Graph showing variation of crystallite size and lattice strain with milling time of ferritic stainless steel (with stearic acid)

4.1.3 Determination of lattice parameter

The lattice parameters of the samples were calculated by XRD analysis with the use of Nelson-Riley function which is given as (equation 2):

$$\frac{\cos^2\theta}{\sin\theta} + \frac{\cos^2\theta}{\theta} \qquad (2)$$

In order to find the lattice parameter a graph was plotted by taking $\frac{\cos^2\theta}{\sin\theta} + \frac{\cos^2\theta}{\theta}$ in x-axis and lattice parameter $\{a=d\ (h^2 + k^2 + l^2)^{1/2}\}$ in y-axis and straight line was obtained. To find the actual lattice parameter the straight was extrapolated to y-axis. The point at which the line intersects the y-axis gives the exact lattice parameter of the powder. Table 4.1 and table 4.2 show

the variation of lattice parameter with milling time for austenitic and ferritic stainless steel (without stearic acid). Table 4.3 and table 4.4 show the variation of lattice parameter with milling time for austenitic and ferritic stainless steel (stearic acid). It can be seen that lattice parameter increases with milling in both cases as Ni and Cr go into the lattice of iron.

Table 4.1 Lattice parameter of austenitic stainless steel (without stearic acid)

Milling Time (hours)	**Lattice Parameter (Å)**
0	3.0584
0.5	3.0673
2	3.0702
5	3.0702
10	3.5487

Table 4.2 Lattice parameter of ferritic stainless steel (without stearic acid)

Milling Time (hours)	**Lattice Parameter (Å)**
0	2.8596
0.5	2.8661
2	2.8661
5	2.8682
10	2.8685

Table 4.3 Lattice parameter of austenitic stainless steel (with stearic acid)

Milling Time (hours)	Lattice Parameter (Å)
0	3.2331
0.5	3.2407
2	3.2914
5	3.750
10	3.4308

Table 4.4: Lattice parameter of ferritic stainless steel (with stearic acid)

Milling Time (hours)	Lattice Parameter (Å)
0	2.8557
0.5	2.8623
2	2.8684
5	2.8701
10	2.8709

4.2 Scanning electron microscopy

Microstructure characterization, morphology and particle size determination was carried by a JEOL JSM-6480 LV scanning electron microscope. Both the secondary electron (SE) mode and back scattered electron mode (BSE) were used as per the requirement. Fig. 4.9 and Fig. 4.10 show the SEM micrographs of austenitic and ferritic stainless steel powder respectively milled for different time periods (without stearic acid). It can be observed that initially particles are

flattened and flake formation is there due to soft nature of powders in both cases. But in later stage, powders are strain hardened, becomes brittle and spherical shape is formed. It is observed that in final stage of milling, powders are agglomerated due to their fineness.

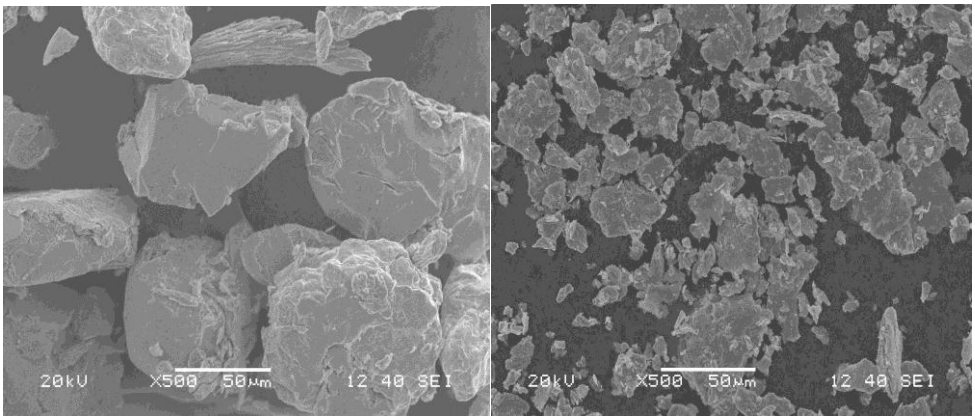

0h **0.5h**

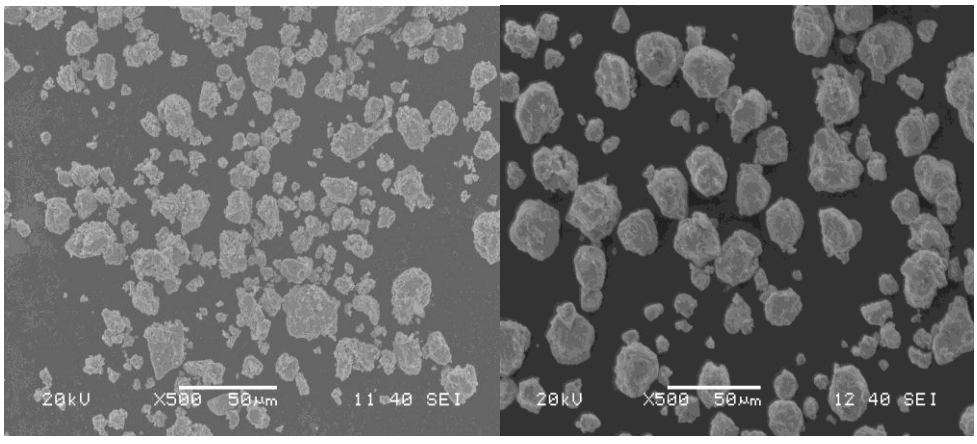

2h **5h**

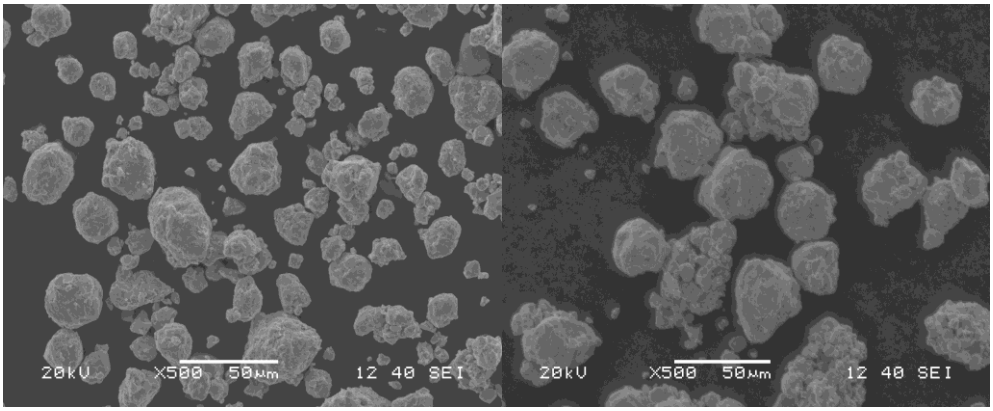

8h **10h**

Fig. 4.9 SEM images of austenitic stainless steel powders milled for 0hr , 30 mins , 2 hr ,5 hr , 8 hr , 10hr (without stearic acid)

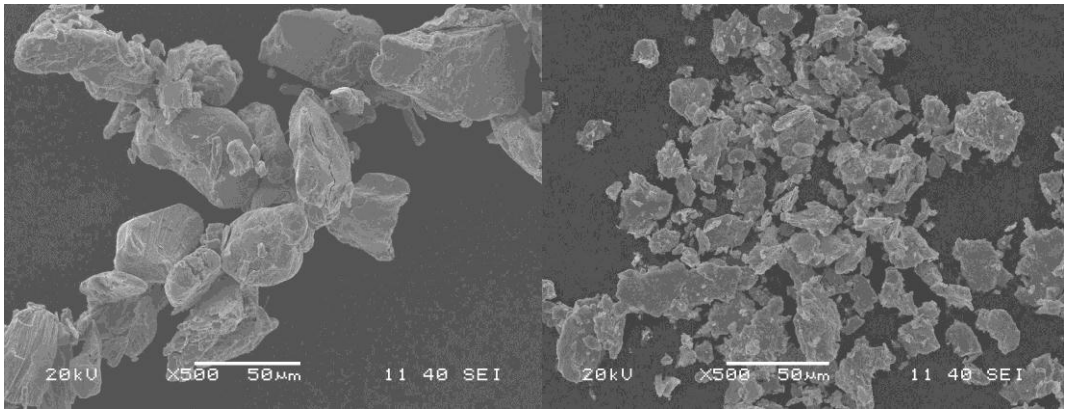

0h **0.5h**

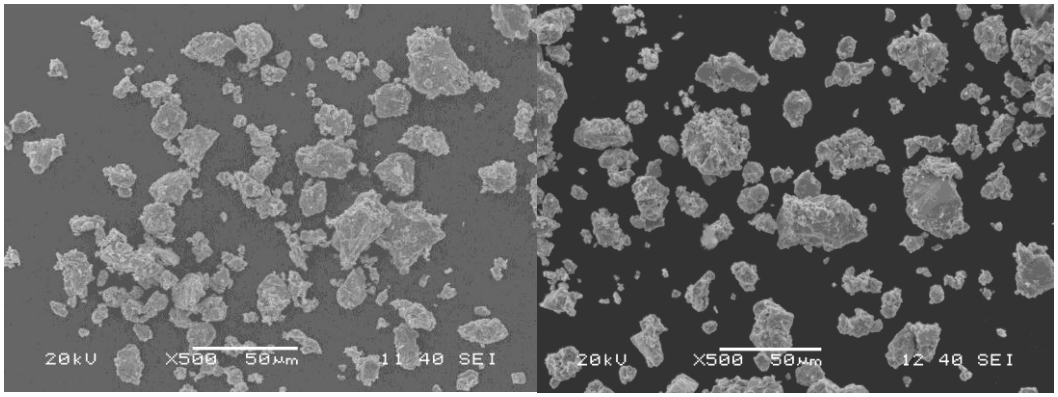

2h **5h**

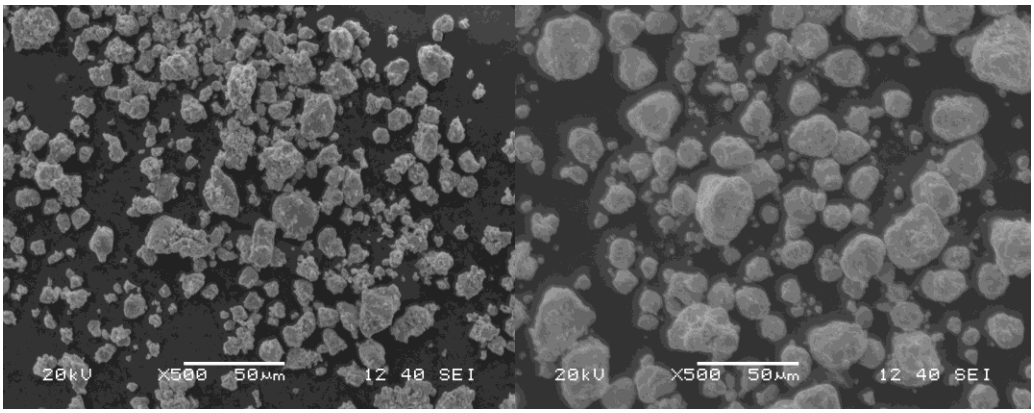

8h **10h**

Fig. 4.10 SEM images of ferritic stainless steel powders milled for 0hr , 30 mins , 2 hr ,5 hr , 8 hr , 10hr(without stearic acid)

Fig. 4.11 and Fig. 4.12 show the SEM micrographs of austenitic and ferritic stainless steel powder milled for various time periods (with stearic acid). It can be observed that initially particles are flattened and flake formation is there due to soft nature of powders in both cases. But in later stage, powders are strain hardened, becomes brittle and spherical shape is formed. The use of stearic acid prevents the formation of spherical structure, rather form flakes. The use of stearic acid also prevents agglomerations of particles and hinders phase transformation. It also results in delay of strain hardening.

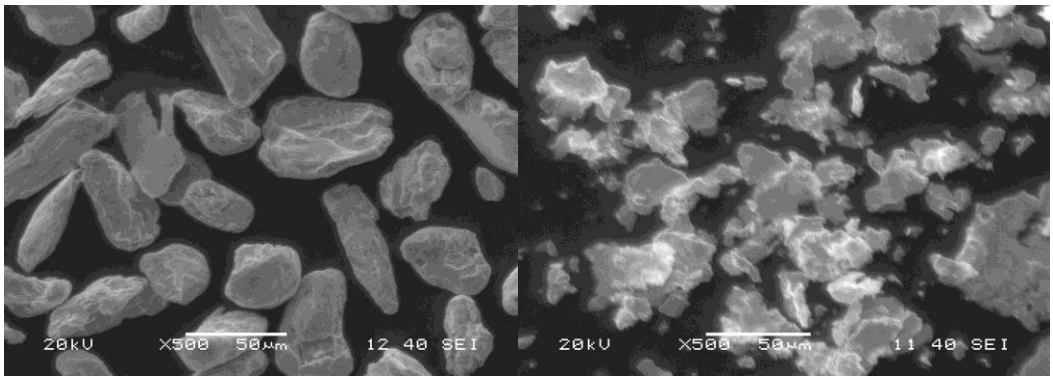

0h **0.5h**

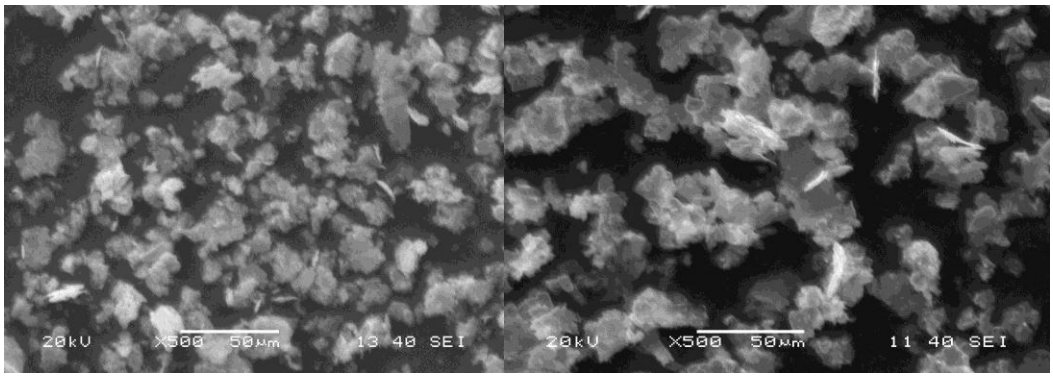

2h **5h**

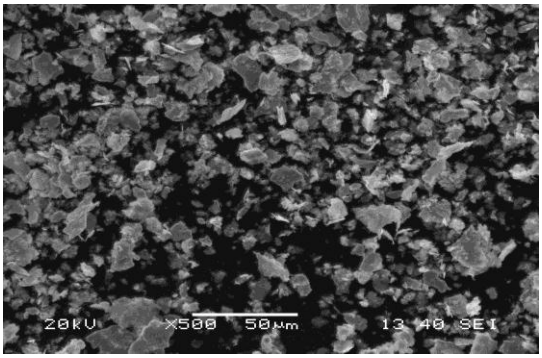

10h

Fig. 4.11 SEM images of austenitic stainless steel powders milled for 0hr , 30 mins , 2 hr ,5 hr , 10hr (with stearic acid)

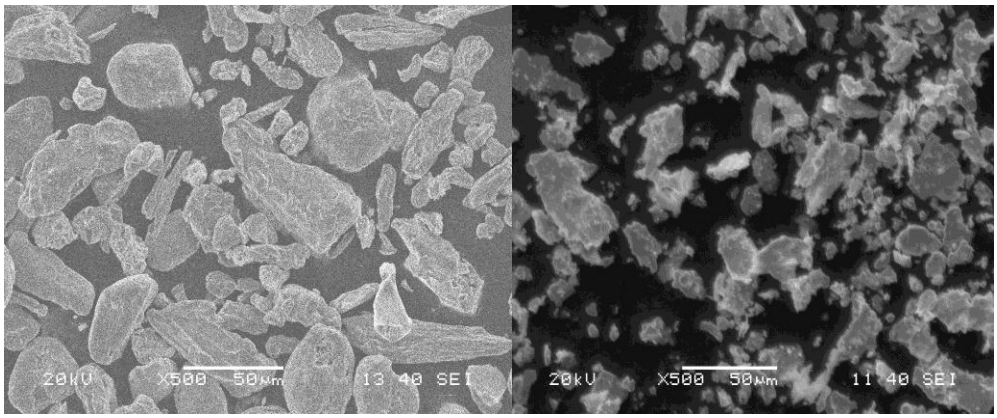

0h **0.5h**

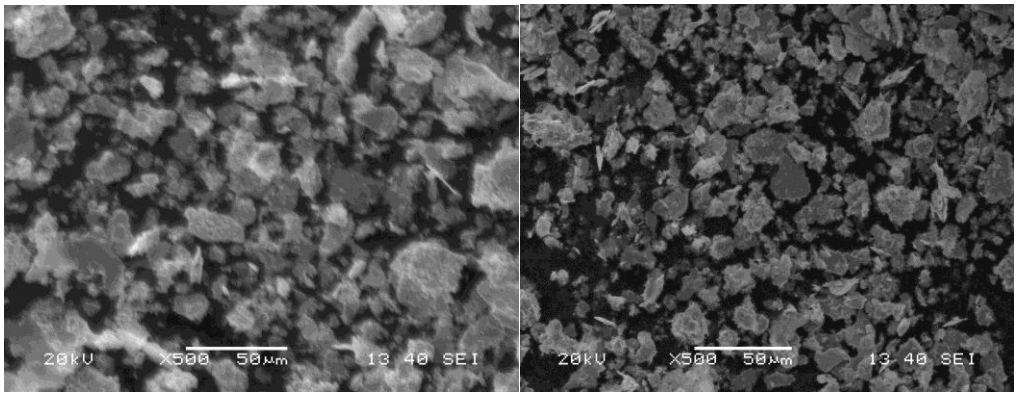

2h **5h**

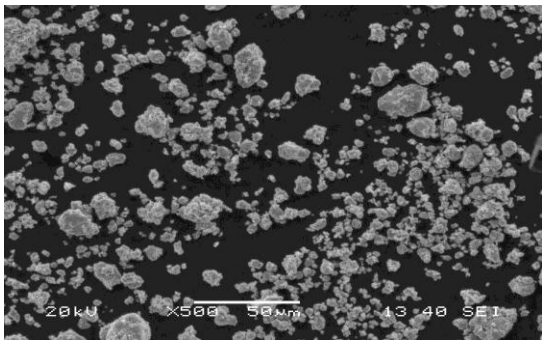

10h

Fig. 4.12 SEM images of ferritic stainless steel powders milled for 0hr , 30 mins , 2 hr ,5 hr , 10hr (with stearic acid)

4.3 Particle Size Analysis

Fig. 4.13 shows the median size plot of austenitic stainless steel powder milled for different time periods. The graph shows that median size decreases with milling. Fig. 4.14 shows the particle size distribution of austenitic stainless steel powder. The graphs show that size distribution curves shift to left side indicating size reduction with milling time.

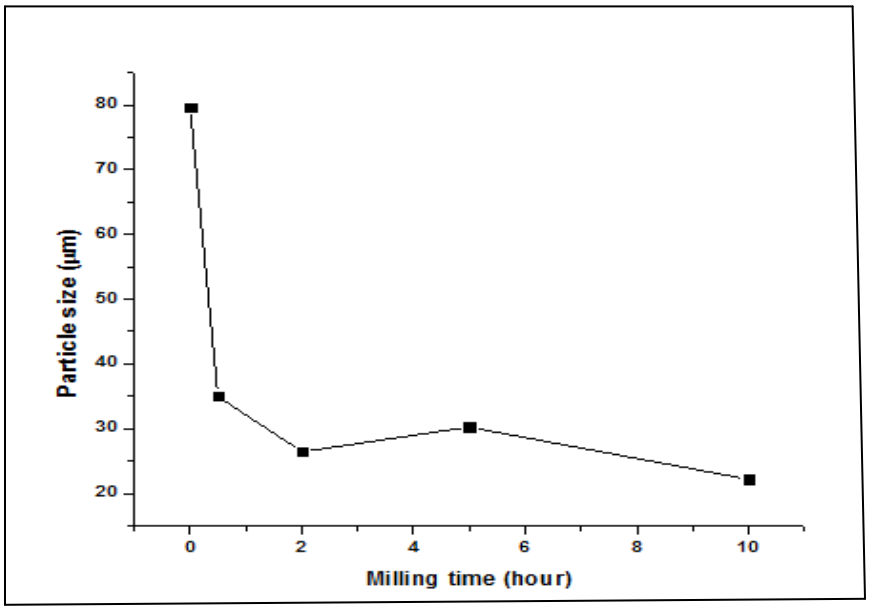

Fig 4.13: Graph showing variation of particle size with milling time for austenitic stainless steel

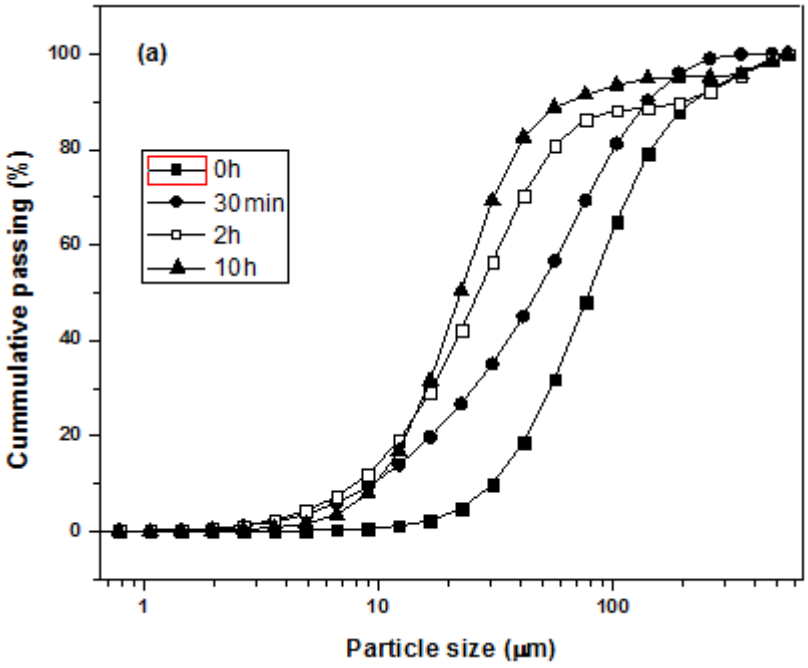

Fig. 4.14 Graph showing particle size distribution of austenitic stainless steel

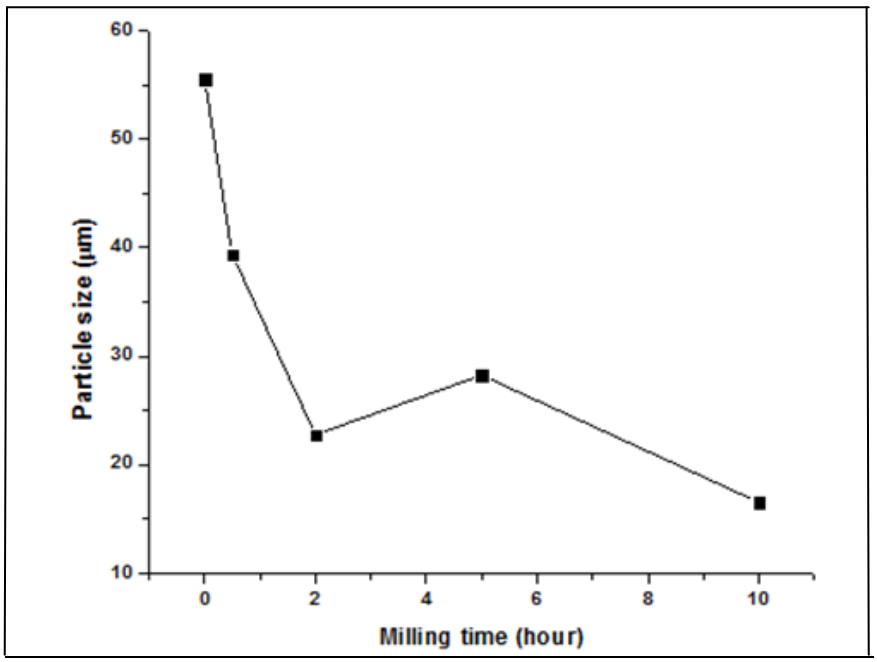

Fig. 4.15 Graph showing variation of Particle size with milling time for ferritic stainless steel

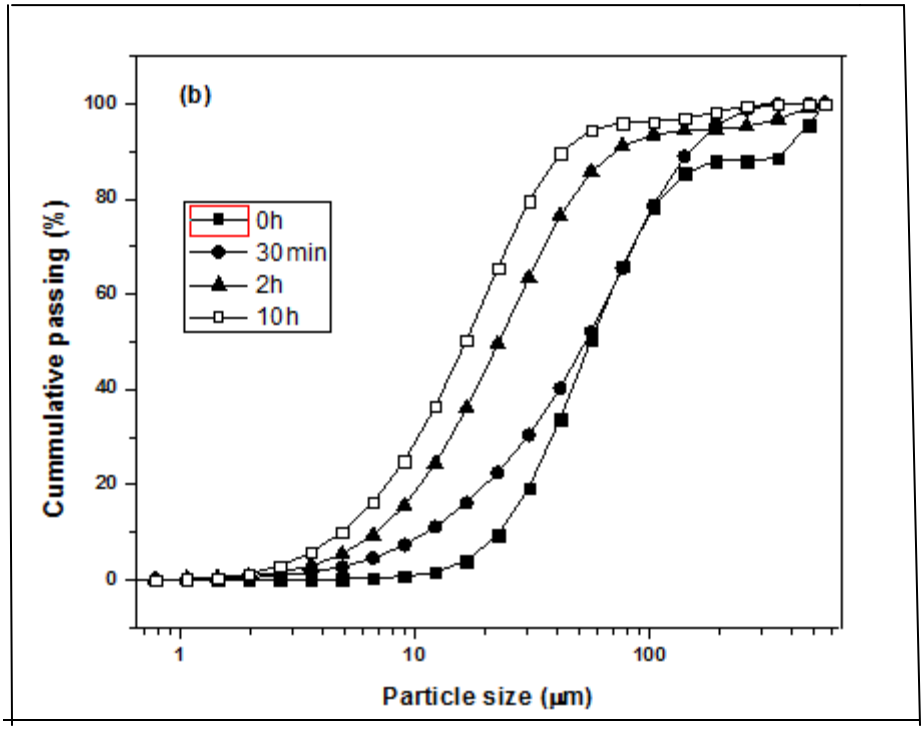

Fig. 4.16 Graph showing particle size distribution for ferritic stainless steel

5. Conclusion

The project report includes a detailed microstructural characterization of austenitic and ferritic stainless steel powders synthesized by mechanical alloying in a high energy planetary mill and determination of crystallite size, lattice strain and lattice parameter. The important conclusions that can be drawn from the results presented here as follows:

- It is possible to synthesis nano-structured stainless steel powder by mechanical alloying by using high energy planetary ball mill.
- As the milling time increases particle size decreases first and then becomes nearly constant afterwards. This is because after a certain interval of time steady state equilibrium is attained between the rate of welding and the rate of fracturing. Welding tends to increase the average particle size while fracturing tends to decrease it.
- It is found that the particle size of alloy powder synthesized goes to the nano range as observed during XRD and SEM studies.
- Crystallite size decreases and the lattice strain increases with increase in the extent of milling.
- Lattice parameter increases with milling time.
- The use of stearic acid prevents the formation of spherical structure, rather form flakes.
- Stearic acid also prevents agglomerations of particles and hinders phase transformation due to formation of a layer on particle surface.

6. Future Scope

This project can be further carried out to get more results and to improve the mechanical properties of stainless steel. Some of the future scope of this project includes:

- Milling parameters can be varied such as ball-to-weight ratio, milling atmosphere and milling speed, etc.
- Annealing of the milled stainless steel powder can be done to study thermal behaviour.
- Consolidation of the stainless steel powder could be done by compaction followed by sintering.
- Other elements can also be added to stainless steel powder to improve mechanical strength of stainless steel.

References

[1] M.H. Enayati, M.R. Bafandeh, J. Alloys Compd, (2007), doi:10.1016/j.jallcom.2007.03.064

[2] D. Oleszak, A. Grabias, M. P¸ekała, A. ´Swiderska-´Sroda, T. Kulik, Journal of Alloys and Compounds, 434–435 (2007) 340–343.

[3] M. Sherif E1-Eskandarany, H.A. Ahmed, Journal of Alloys and Compounds, 216 (1994) 213-220.

[4] T. Haghir, M.H. Abbasi, M.A. Golozar, M. Panjepour, Materials Science and Engineering *A*, 507 (2009) 144–148.

[5] K.J. Kurzydłowski, Bull. Pol. Acad. Sci., Tech. Sci. 52 (4) (2004) 275.

[6] J. Ding, H. Huang, P.G. McCormick, R. Street, J. Magn. Magn. Mater. 139 (1995) 109.

[7] Yamada K, Koch CC. J Mater Res 1993;8:1317±26.

[8] Szymanski K, Zaleski P, RecÂko K, Waliszewski J. Mater Sci Forum1997:235-238:223-8

[9] Basset D, Matteazzi P, Miani F. Mater Sci and Engng 1993;A168:149-52.

[10] Kimura H, Kimura M, Takada F. J Less-Common Metals 1988;140:113-8.